Investigation of Remote Sensing Imageries for Identifying Soil Texture Classes Using Classification Methods

Wei Wu, Qipo Yang, Jiake Lv, Aidi Li, and Hongbin Liu

***Abstract*— In this paper, the usefulness of remote sensing imageries for identifying soil texture classes was evaluated by classification trees under one-against-one (OAO), one-against-all, and all-together schemes. A set of normalized difference vegetation indices (NDVIs) was obtained from cloud-free Landsat images over a small mountainous watershed. Terrain indicators (elevation, slope, and topographic wetness index) were derived from a digital elevation map (30 m). Models with different input parameters (purely NDVI, purely topography and stratum, and NDVI plus topography and stratum) were developed. Overall accuracy, kappa statistic, receiver operating characteristics (ROC), and the area under ROC curve (AUC) were applied to evaluate the classification accuracy. Results showed that the classification strategy had great effects on the outputs. The models under OAO scheme performed better with averaged overall accuracy, kappa statistic, and AUC of 0.949, 0.821, and 0.87, respectively. Among them, the model with NDVI plus topography and stratum performed best with overall accuracy, kappa statistic, and AUC of 0.975, 0.918, and 0.907, respectively. Similar performances were obtained by the model with purely NDVI and the model with purely topography and stratum. More samples of clay and sand were identified with the help of NDVI. The contributions of NDVI to explain soil texture class variability were 144%, 0%, and 14% for clay, loam, and sand, respectively. NDVI measured during the stem and leaf growth period of sweet potatoes was the optimum period for identifying soil texture classes in the watershed. Our findings will provide valuable information for assessing the quality of ecological environment using remote sensing data.**

***Index Terms*— All-together, comparison, one-against-all (OAA), one-against-one (OAO), optimum period, pattern classification.**

I. Introduction

SOIL texture plays a critical role in determining soil water holding capacity and hydraulic properties and consequently affects soil nutrient regime, soil fertility, and plant growth and development [1]. Soil spectral reflectance is closely related with soil physical and chemical properties (e.g., particle size, surface roughness, soil organic, and moisture) [2]. Therefore, remote sensing data could be used for estimating soil texture at topsoil [3]. Normalized difference vegetation index (NDVI), a widely used vegetation index, has been applied to explore the relationship between soil texture and vegetation around the world [4]–[6]. For example, clay-rich soils had higher NDVI values in Botswana [4] and southeastern Iran [3]. In South Texas High Plains of USA, NDVI was negatively correlated with clay content and positively correlated with sand content [7]. Recently, several works demonstrated that remote sensing data could be used to predict soil surface texture [5], [6]. NDVI and the digital number of bands 2, 3, 5, and 7 could explain most of the variability of the soil texture [6]. However, the investigation of the relationship between NDVI and soil texture classes also could be a classification task. Thus, we assume NDVI measured by sensors might be useful in identifying soil texture classes.

Multiclass classification aims to deal with tasks with more than two classes. It has been widely applied to information retrieval, speech recognition, text categorization, and land cover or land use classification of remote sensing data [8]–[13]. Generally, multiclass classification focuses on modeling accurate classifiers with one-against-one (OAO), one-against-all (OAA), or all-together strategies. Some approaches, for example, the well-known support vector machines (SVMs), decompose a multiclass classification problem into multiple binary class problems using OAO or OAA schemes [11], [14]. Previous studies reported that classification systems with OAO scheme performed better than that with OAA strategy [8], [11], [15]–[17]. For instance, the SVMs with OAO scheme gave much higher accuracy than that with OAA scheme for identifying foreign fibers in cotton lint [15]. El-Bendary *et al.* [11] compared SVMs and linear discriminant analysis to investigate tomato ripeness stages using color features. Their experimental results showed that the SVM with OAO scheme performed better than the SVM with OAA scheme and linear discriminant analysis. However, the performances of classifiers with different schemes are application-dependent [8], [17]. For example, Ou and Murphey [8] evaluated multiclass pattern classification using six different artificial neural networks (ANNs) with OAA, OAO, one-against higher order, and P-against-Q strategies based on well-known benchmark data. They concluded that the neural network with OAA scheme performed well for small training data sets while the neural network with OAO scheme performed better for huge training data sets.

Manuscript received April 4, 2018; revised July 22, 2018; accepted August 14, 2018. This work was supported by the National Key Research and Development Program of China under Grant 2018YFD0200500. *(Corresponding author: Hongbin Liu.)*

W. Wu and J. Lv are with the College of Computer and Information Science, Southwest University, Chongqing 400716, China (e-mail: wuwei_star@163.com; lvjiake@qq.com).

Q. Yang, A. Li, and H. Liu are with the College of Resources and Environment, Southwest University, Chongqing 400716, China (e-mail: 2316387911@qq.com; 9196201@qq.com; lhbin@swu.edu.cn).

Color versions of one or more of the figures in this paper are available online at http://ieeexplore.ieee.org.

Digital Object Identifier 10.1109/TGRS.2018.2868141

Recently, many approaches, such as conventional statistical analyses and machine-learning algorithms, have been applied to deal with the classification tasks in digital soil mapping, and comparative studies indicated that models performed differently under varied circumstances [9], [10], [12], [18]. For instance, SVMs outperformed ANNs for classifying rock layers using ground penetrating radar data [9]. Wu *et al.* [19] also found that SVMs gave much higher performance than ANN and classification tree (CT) for classifying soil texture classes based on terrain indicators. However, an opposite result was reported by Taghizadeh-Mehrjardi *et al.* [18]. The authors applied SVM, *k*-nearest neighbor, random forest, logistic regression, ANN, and CT model to estimate the spatial distribution of soil groups in Iran. The comparative results indicated that CT model and ANN performed better with higher values of overall accuracy and kappa statistic.

Among the approaches aforementioned, decision tree methods are gaining favor in various fields for exploring nonlinear relationships between the independent and response variables [20]. They help researchers make a choice between several options. Decision trees are nonparametric method and easy to build and interpret. They can automatically handle both continuous and categorical variables. In addition, decision trees provide the relative importance of each independent variable to the target one. The models are scalable to large problems and can handle smaller data set than ANNs [21]. Classification and regression tree (CART) is a typical decision tree algorithm for predicting continuous variable (regression) or categorical variable (classification). A particular benefit of CART is its cross-validation feature that attempts to detect overfitting [20].

In consideration of the advantages of CART and the accessibility of NDVI, we attempted to: 1) examine the usefulness of NDVI for identifying soil texture classes; 2) improve the performance of CTs; and 3) investigate the optimum period of NDVI for detecting soil texture classes. Hence, three models with different input parameters (purely NDVI, purely topography and stratum, and NDVI plus topography and stratum) were compared to determine the role of NDVI for contributing to explain soil texture class distribution with respect to the effects of environmental variables (e.g., topography and stratum [19], [22]–[25]) on soil texture class variability. The work was done using CTs under OAO, OAA, and all-together strategies. The results are expected to provide useful information for assessing the quality of ecological environment using remote sensing data.

II. Materials

The study site covers 5376 ha and is located in southwest China (Fig. 1). The climate is moderate subtropic with a mean temperature of 15 °C, a relative humidity of 75%, the sunlight of 1477 h, and a mean annual precipitation of 1224 mm, which mainly occurs in May–September. Long-term mean temperature and precipitation had low spatial variability with coefficients of variation of 9.59% and 1.73%, respectively. The topography is mountains with elevation varying between 241 and 1582 m and slope ranging between 0 and 108%. Main land use types are forest and dryland which account for

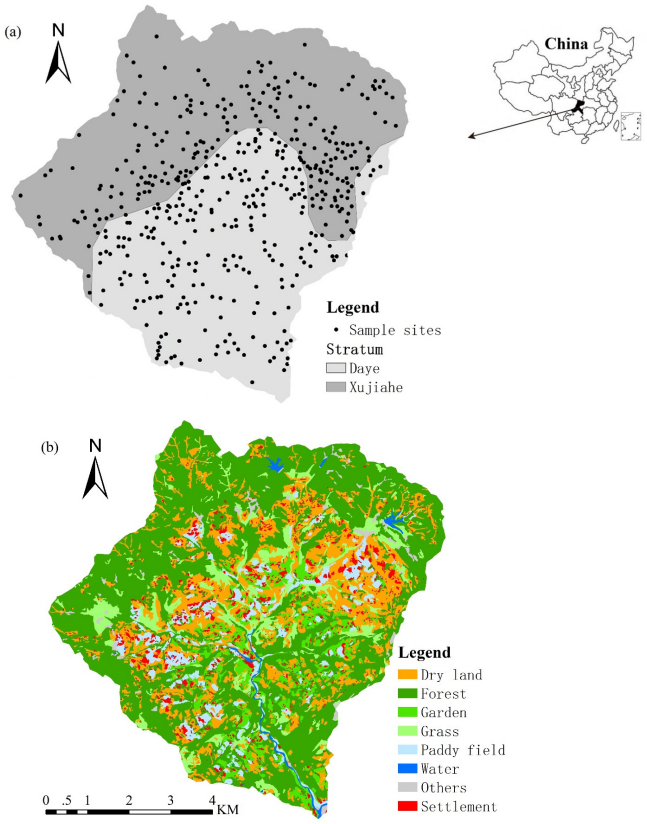

Fig. 1. Maps of (a) location, sample sites, stratum, and (b) land use types of the study area.

51.3% and 20.8% of the total area, respectively. For dryland, the crop rotation is winter rapeseed (*Brassica napus* L.), corn (*Zea mays* L.), or sweet potato (*Ipomoea batatas* L.). Corn was planted in April and harvested in July. Sweet potato was planted in June and harvested in October. Winter rapeseed was planted in October and harvested in April. For each crop, agro-techniques and variety were the same.

The dominant geology includes two soil strata, which were deposited in the early Triassic period (Daye formation) and mid-late Triassic period (Xujiahe formation) [26]. Soils developed from the two geological units are classified as Regosols and Entisol, respectively [26]. The soil is neutral with pH varying between 5.3 and 8.6 and organic matter ranging between 6.3 and 26 g/kg.

In order to obtain cloud-free images covering spring, summer, autumn, and winter seasons, the images from Landsat 5 and 8 with 30-m spatial resolution were acquired since 2011. Finally, four image data sets on April 26, 2011 (DOY 116, representing spring), September 1, 2011 (DOY 244, representing summer), October 11, 2014 (DOY 284, representing autumn), and December 17, 2015 (DOY 351, representing winter) which were cloud-free over the entire region were used in this paper (Fig. 2).

To generate consistent and high-quality image materials, preprocessing including radiometric calibration and atmospheric correction are needed. In this paper, they were done by the environment for visualizing images (ENVIs).

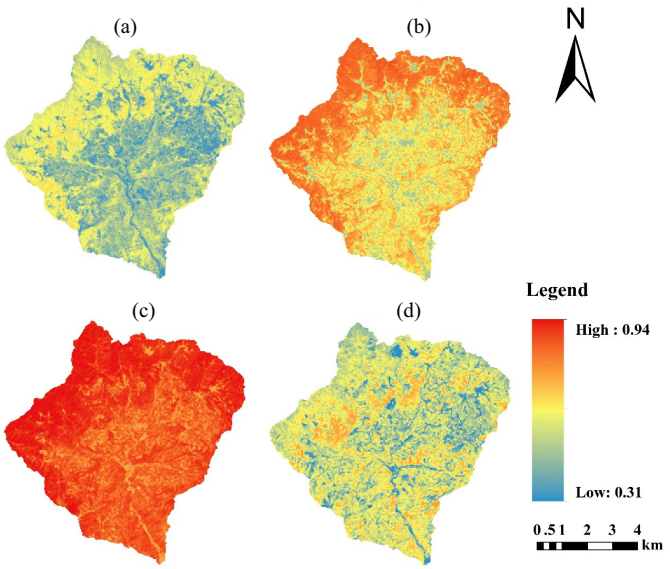

Fig. 2. Four images of NDVI over the study site. (a) DOY 116, spring. (b) DOY 244, summer. (c) DOY 284, autumn. (d) DOY 351, winter.

大气校正、光谱超立方体与ENVI耦合的快速视线大气分析

An atmospheric correction model, fast line-of-sight atmospheric analysis of spectral hypercube coupled with ENVI, was performed on the four images. Then, the four images were clipped to the study area. The NDVI which is a widely used vegetation index is calculated for each pixel by red (P_{red}, band 3 for Landsat 5 and band 4 for Landsat 8) and near infrared (P_{nir}, band 4 for Landsat 5 and band 5 for Landsat 8) values using the following equation [27], [28]:

$$\text{NDVI} = \frac{P_{\text{nir}} - P_{\text{red}}}{P_{\text{nir}} + P_{\text{red}}}. \quad (1)$$

Finally, NDVI values of the four images were extracted to the soil samples using ArcGIS software v10.0.

The data of soil texture classes (clay, loam, and sand) introduced by Wu *et al.* [19] were used in this paper. A total of 1032 soil samples (20 cm, topsoil) were collected from drylands in September 2012. Ten subsamples were randomly collected from each field and mixed as a composite sample. Soil texture class was then estimated by twisting the composite sample according to the flowchart recommended by Thien [29] and FAO [30]. This approach is known as "texture-by-feel" or "Fingerprobe" [31], and it is regarded as an appropriate alternative to the determination of soil texture in the laboratory [32]–[35].

In order to assess the estimated texture classes by Fingerprobe in field, the soil particle sizes of 43 samples were analyzed in the laboratory using the pipette method. Their soil texture classes were then determined by soil texture calculator (https://www.nrcs.usda.gov/wps/portal/nrcs/detail/soils/survey/?cid=nrcs142p2_054167). The overall accuracy and kappa index of the classes (clay, loam, and sand) measured by the experienced soil scientists in the field and by the lab analyses were 76.7% and 0.604, respectively. Hence, the data were suitable for further analyses. Detailed information about the procedure of soil texture class measurement could be found in [19].

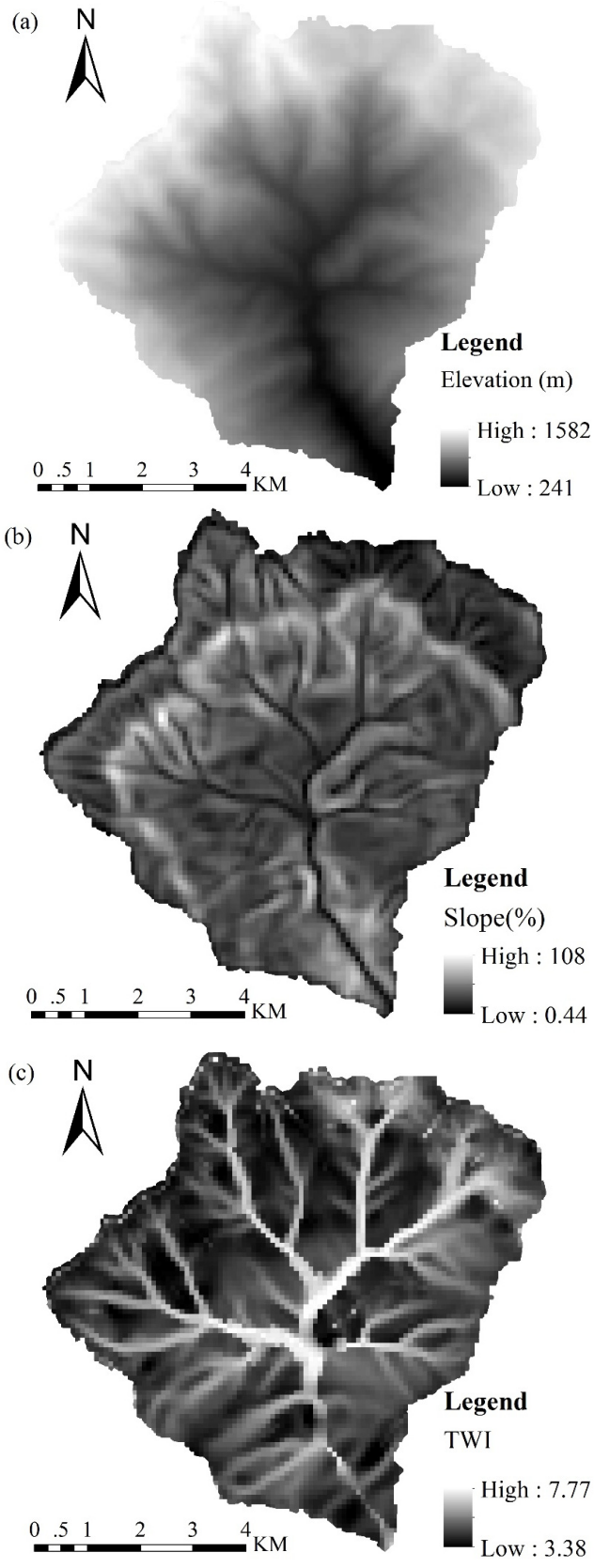

Fig. 3. (a) Digital elevation map, (b) slope, and (c) TWI of the study area.

An elevation map (global digital elevation model) with a resolution of 30 m was used in this paper. Fig. 3 shows the three terrain indicators [elevation, slope, and topographic

wetness index (TWI)], which were calculated by the system for automated geoscientific analyses software v2.1.4 [36].

In order to avoid the effect of the mixed pixels on the classification accuracy, the pixels that correspond to the pure dryland plots were used. If the dryland plot had several pixels, the mean value of NDVIs was calculated. This was done by the ArcGIS software v10.0. Finally, the sample numbers of clay, loam, and sand soil texture classes were 28, 384, and 62, respectively. For the Xujiahe formation, the sample numbers were 7, 210, and 22 for clay, loam, and sand soil texture classes, respectively. For Daye formation, the sample numbers were 21, 174, and 40 for clay, loam, and sand soil texture classes, respectively.

III. Methodology

A. Classification Tree

CART was introduced by Breiman *et al.* [20] in 1984. It is a nonparametric method. Based on recursive partitioning rules, CART creates a binary tree for users to make a decision [37]. The response and predictors could be continuous or categorical variables. In this paper, the CT was applied to investigate the ability of NDVI for identifying soil texture classes. Gini index, which is a widely used measure, was applied to split the data [38]

$$\text{Gini}(N) = 1 - \sum_{i=1}^{k} (p(c_i))^2 - \sum_{i=1}^{n} p(t_i) \sum_{j=1}^{k} \times p(c_j \mid t_i)(1 - p(c_j \mid t_i)) \quad (2)$$

where N is a test with n outcomes. A test that maximizes the function is selected by the Gini index. For a node (t), a sample is allotted to a class (c_i) with the probability $p(c_i|t)$ based on an impurity function which is calculated by the Gini index. When the sample is really allotted to class c_j, the probability is $p(c_j|t)$.

One output of CART is the relative importance of variables. The calculation of this is based on the improvement measure of the variable for the construction of the tree. For each variable, the values of all the improvements are summed over each node and are then scaled relative to the best performing variable. The variable with the highest sum of improvements is scored 100, and all other variables will have lower scores ranging downward toward 0 [20]. The minimum numbers of parent nodes and child nodes were 3 and 1 in this paper, respectively. The maximum tree depth was 5.

B. Classification Scheme

Three schemes, namely, all-together, OAA, and OAO, were adopted in this paper. In the all-together scheme, one CT was built using all samples. In the OAA scheme, the ith class is trained against all other classes by a CT, and k trees are built for k classes. In the OAO scheme, the ith class is trained against every other class, and $k(k-1)/2$ CTs are built to train each pair of the classes $[(1,2),(1,3),\ldots,(1,i),\ldots,(1,k-1),(1,k),(2,3),\ldots,(2,i),\ldots,(2,k),\ldots,(k-1,k)]$. For the scheme which produces abundant results, such as OAO method, an extension of the majority vote method considering the probability for an input vector generated by the CTs is applied to determine the final class

$$F(x) = \arg\left\{ \sum_{j=1}^{m-1} (1-p_{j,m}) + \sum_{j=m+1}^{K} p_{m,j} \mid m = 1, 2, \ldots, K \right\} \quad (3)$$

where $p_{i,j}$ is the probability of the input vector x being class i and $(1-p_{i,j})$ is the probability of the input vector x being class j for any $i = 1, 2, \ldots, K-1$ and $j = i+1, i+2, \ldots, K$.

Three data sets were created for the study. The first one was purely NDVI data of the four seasons. The second database contained purely terrain indicators and stratum. The third one was composed of NDVI, terrain indicators, and stratum. Therefore, models with different data sets (purely NDVI, purely terrain indicators and stratum, and NDVI complemented with terrain indicators and stratum) were developed and compared under the three schemes.

C. Performance Evaluation

To avoid overfitting, the tenfold cross-validation was applied to examine the model performance [39]–[41]. Samples were randomly separated into 10 subsets. Each subset contains all the three soil texture classes. The model performance was evaluated by overall accuracy, kappa statistic, receiver

TABLE I

Analysis of One-Way Variance for NDVI Values and Terrain Parameters Among Soil Texture Classes and Between Strata

	Soil texture class			Stratum	
	Clay	Loam	Sand	Daye	Xujiahe
NDVI					
DOY 116	0.4607b	0.4795b	0.5091a	0.473b	0.4914a
DOY 244	0.6449b	0.6764a	0.6906a	0.6506b	0.7018a
DOY 284	0.8502b	0.8594b	0.8746a	0.85b	0.8716a
DOY 351	0.5476b	0.5421b	0.5906a	0.5554a	0.5422a
Mean	0.6259b	0.6394b	0.6663a	0.6323b	0.6518a
Terrain					
Elevation	767b	888a	830ab	715b	1029a
slope	34a	37a	40a	34b	39a
SAGATWI	4.70ab	4.87a	4.49b	4.88a	4.74b

Letters indicate significant differences among columns (soil texture class columns and stratum columns, ANOVA, $p < 0.05$ according to least significant difference post-hoc analysis).

TABLE II

Pearson's Coefficients Between NDVI and Terrain Indicator

	DOY116	DOY244	DOY284	DOY351
Elevation	0.295**	0.591**	0.488**	-0.013
Slope	0.221**	0.122**	0.196**	0.155**
TWI	-0.112*	-0.053	-0.187**	-0.133**

* and **: Significance level at $p < 0.05$ and $p < 0.01$, respectively.

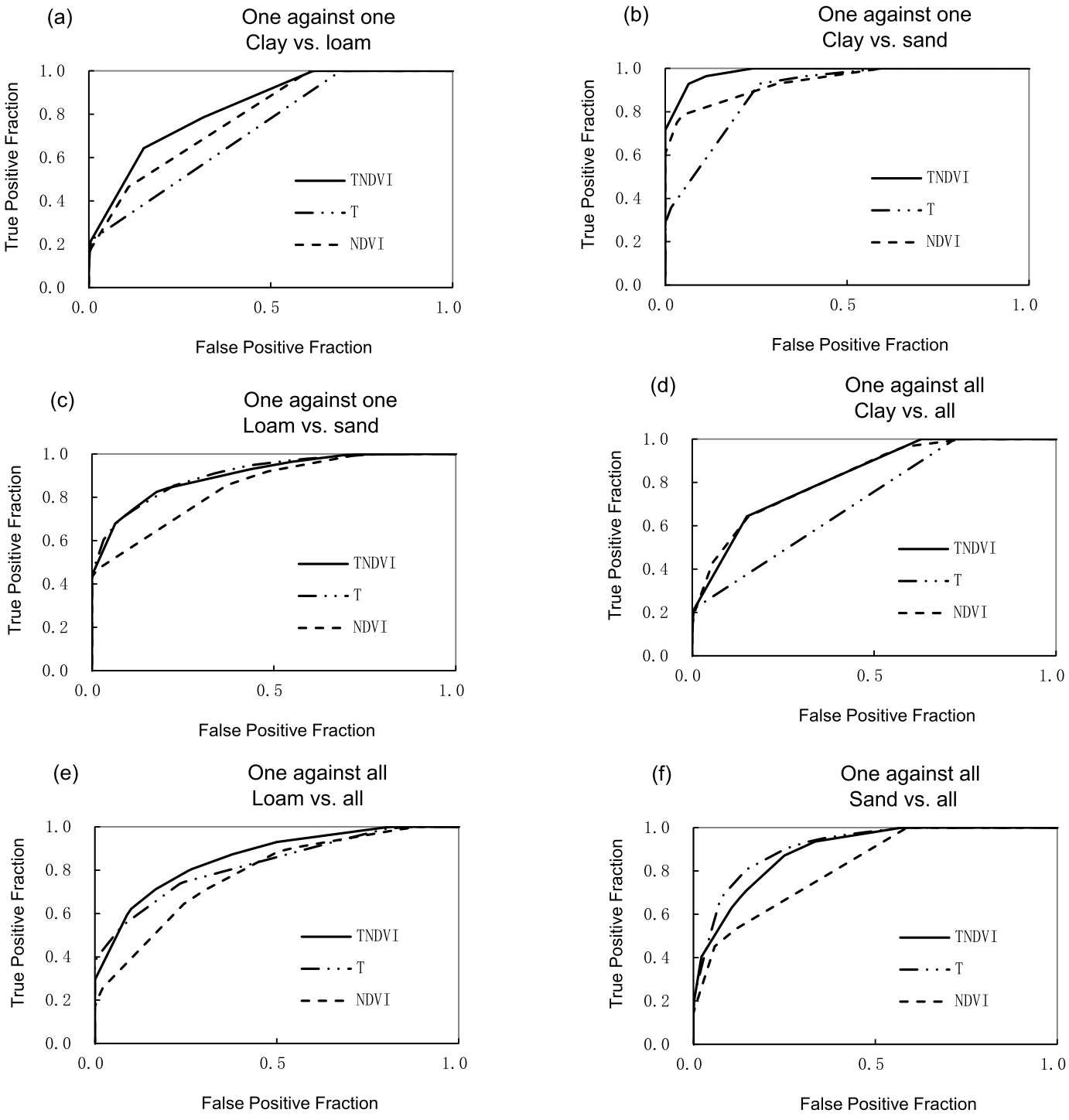

Fig. 4. ROC curves of models with different input parameters (TNDVI: NDVI plus terrain indicators and stratum; T: terrain indicators and stratum; and NDVI: purely remote sensing imageries) under (a)–(c) OAO, (d)–(f) OAA, and (g)–(i) all-together schemes.

operating characteristics (ROCs), and the area under the ROC curve (AUC). In terms of kappa statistic, the model performs poor (<0), slight (0–0.2), fair (0.21–0.4), moderate (0.41–0.6), substantial (0.61–0.8), and excellent (0.8–1) [42]. AUC varies between 0 and 1. It is one of the most popular measures for imbalanced classes [43]. A value of AUC close to 1 indicates a better performance. An AUC value of 1 indicates a perfect model, while an AUC value of 0 indicates a noninformative model. According to Kantardzic [43], the model performs excellent (0.9–1), very good (0.8–0.9), good (0.7–0.8), average (0.6–0.7), and poor (0.5–0.6).

The relative improvements of overall accuracy, kappa statistic, and AUC were used to measure the improvement on the classification accuracy of an evaluated model over the reference methods

$$\mathrm{RI} = \frac{I_E - I_R}{I_R} \tag{4}$$

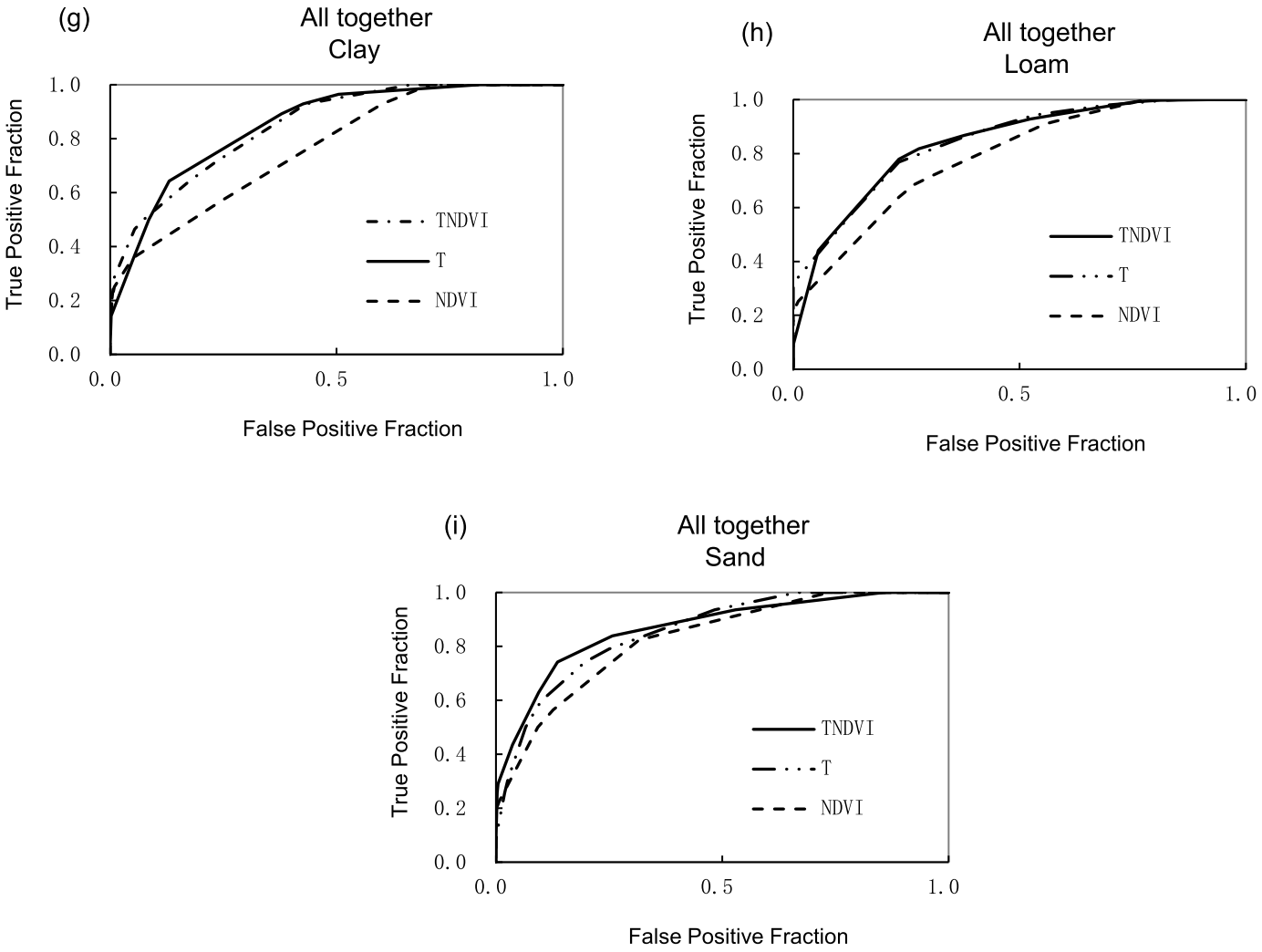

Fig. 4. *(Continued.)* ROC curves of models with different input parameters (TNDVI: NDVI plus terrain indicators and stratum; T: terrain indicators and stratum; and NDVI: purely remote sensing imageries) under (a)–(c) OAO, (d)–(f) OAA, and (g)–(i) all-together schemes.

where I_E and I_R are the accuracy indicators for the evaluated and reference models, respectively.

D. Statistical Analysis

A one-way analysis of variance (ANOVA) with Fisher's least significant difference procedure was used to test the difference in NDVI and terrain indicators among soil texture classes and strata. Pearson's correlation coefficients were calculated to determine the strength of correlations between NDVI and terrain indicators. The analyses were performed in SPSS v13.0 and MATLAB v9.0.

IV. Results and Discussion

A. Basic Statistics

NDVI values varied with the soil texture classes and the growth stages. Highest values of NDVI were found in the middle of October (DOY 284) when the drylands were covered with sweet potato leaves. Lowest values of NDVI were found in the end of April (DOY 116) when corn plants were transplanted. The results of ANOVA indicated that mean differences in NDVI were observed among the soil texture classes (Table I). These confirmed the strong relationships existing between NDVI values and soil texture classes [4], [5], [7], [44]. On average, NDVI values were highest for sand soils and lowest for clay soils over the study site ($p < 0.05$). Li *et al.* [7] also found that NDVI was lower in the areas where soils contained more clay but less sand. This might be that water use efficiency was reduced significantly when crops were grown in clayey soils and hence influenced plant growth and development [45], [46]. However, Farrar *et al.* [4] reported that higher NDVI values were observed in clay-rich soils, which was opposite with our finding. This indicated that varied relationships between NDVI and soil texture existed around the world.

According to the results of ANOVA, the two strata also had significant differences in NDVI values (Table I). For the Xujiahe formation, the averaged NDVI and NDVIs measured at DOY 116, DOY 244, and DOY 284 were 3.01%, 3.81%, 7.85%, and 8.88% higher than that of the Daye formation.

Moreover, significant differences in terrain parameters were found among soil texture classes and between strata (Table I).

TABLE III

AUC OF THE MODELS WITH DIFFERENT INPUT PARAMETERS UNDER OAO, OAA, AND ALL-TOGETHER SCHEMES

		TNDVI	T	NDVI	Mean
All together	Clay	0.851	0.849	0.767	
	Loam	0.840	0.845	0.789	
	Sand	0.869	0.858	0.829	
	Mean	0.853	0.851	0.795	0.833
OAA					
	Clay vs. all	0.828	0.715	0.829	
	Loam vs. all	0.859	0.827	0.78	
	Sand vs. all	0.893	0.912	0.82	
	Mean	0.86	0.818	0.81	0.829
OAO					
	Clay vs. loam	0.833	0.727	0.792	
	Clay vs. sand	0.984	0.892	0.939	
	Loam vs. sand	0.903	0.908	0.848	
	Mean	0.907	0.842	0.860	0.87

TNDVI: NDVI plus terrain indicators and stratum; T: only terrain indicators and stratum.

TABLE IV

CONFUSION MATRIX FOR THE MODELS WITH DIFFERENT INPUT PARAMETERS BASED ON OAO SCHEME

		Clay	Loam	Sand	Overall accuracy	Kappa
NDVI	Clay	14	14	0	0.939	0.781*
	Loam	0	384	0		
	Sand	0	15	47		
T	Clay	9	18	1	0.935	0.764*
	Loam	0	384	0		
	Sand	0	12	50		
TNDVI	Clay	22	6	0	0.975	0.918*
	Loam	0	383	1		
	Sand	0	5	57		
Mean					0.949	0.821

*: significant at $P < 0.05$. TNDVI: NDVI plus terrain indicators and stratum; T: purely terrain indicators and stratum.

TABLE V

CONFUSION MATRIX FOR THE MODELS WITH DIFFERENT INPUT PARAMETERS BASED ON OAA SCHEME

		Clay	Loam	Sand	Overall accuracy	Kappa
NDVI	Clay	6	20	2	0.84	0.26*
	Loam	0	383	1		
	Sand	0	53	9		
T	Clay	6	17	5	0.852	0.356*
	Loam	0	383	1		
	Sand	0	47	15		
TNDVI	Clay	10	18	0	0.869	0.435*
	Loam	0	384	0		
	Sand	0	44	18		
Mean					0.854	0.35

*: significant at $P < 0.05$. TNDVI: NDVI plus terrain indicators and stratum; T: purely terrain indicators and stratum.

Clayey soils were mainly located in the lower areas with higher values of TWI. Sandy soils were mostly located in the areas with steeper slopes, which were 9.76% and 7.14% higher than that of clayey and loamy soils ($p < 0.05$). Compared to the Xujiahe formation, the Daye formation was mostly concentrated in lower areas with lower values of slope and higher values of TWI.

NDVIs were positively correlated with slope and negatively correlated with TWI ($p < 0.01$, Table II). NDVIs at DOY 116, DOY 244, and DOY 284 were positively correlated with elevation over the study site ($p < 0.01$). This was opposite with the results reported by Li *et al.* [7]. They found that NDVI was negatively correlated with elevation.

B. Model Performance

The classification accuracy of the models with different input parameters under all-together, OAA, and OAO schemes was evaluated using ROC curves (Fig. 4). Their corresponding AUC values are calculated and given in Table III. The overall values of AUC of the models for all-together, OAA, and OAO schemes were 0.833, 0.829, and 0.87, respectively. Clearly, models under OAO scheme outperformed that under all-together and OAA schemes.

The confusion matrix, overall accuracy, and kappa statistic produced by the developed models with different input parameters under OAO, OAA, and all-together schemes are shown in Tables IV–VI. The mean values of overall accuracy and kappa statistic were 0.949 and 0.821 for the models under OAO scheme, 0.854 and 0.35 for the models under OAA scheme, and 0.845 and 0.304 for the models under all-together scheme, respectively. According to kappa statistic, the model under OAO scheme gave excellent agreement, while the models under all-together and OAA schemes gave fair agreement. The relative improvements in overall accuracy and kappa statistic of the model under OAO scheme over that under all-together and OAA schemes were 12.3% and 170%, and 11.1% and 135%, respectively. These further confirmed that models under OAO scheme outperformed that under all-together and OAA schemes. Similar results of overall accuracy and kappa statistic were obtained by the models under all-together and OAA schemes. The relative improvements in overall accuracy and kappa statistic of the models under OAA scheme over that under all-together scheme were 1.1% and 15.1%, respectively. The outcomes of this paper were in agreement with [8] and [11]. They also found that OAO scheme performed better than OAA and P-against-Q schemes for multiclass pattern classification using SVMs and ANNs. These results indicated that the classification strategy had great effects on the outputs.

TABLE VI

CONFUSION MATRIX FOR THE MODELS WITH DIFFERENT INPUT PARAMETERS BASED ON ALL-TOGETHER SCHEME

		Clay	Loam	Sand	Overall accuracy	Kappa
NDVI	Clay	3	25	0	0.838	0.223*
	Loam	0	384	0		
	Sand	0	52	10		
T	Clay	8	19	1	0.844	0.342*
	Loam	0	378	6		
	Sand	3	45	14		
TNDVI	Clay	4	24	0	0.854	0.349*
	Loam	0	383	1		
	Sand	0	44	18		
Mean					0.845	0.304

*: significant at $P < 0.05$. TNDVI: NDVI plus terrain indicators and stratum; T: purely terrain indicators and stratum.

TABLE VII

MODEL PERFORMANCE BASED ON MIXED PIXELS

Scheme		Overall accuracy	Kappa	Mean AUC
All together	NDVI	0.845	0.218	0.746
	T	0.843	0.153	0.808
	TNDVI	0.854	0.289	0.807
	Mean	0.847	0.22	0.77
One against all	NDVI	0.849	0.231	0.77
	T	0.855	0.273	0.793
	TNDVI	0.87	0.385	0.807
	Mean	0.858	0.296	0.79
One against one	NDVI	0.927	0.708	0.829
	T	0.931	0.724	0.814
	TNDVI	0.955	0.835	0.841
	Mean	0.938	0.756	0.828

TNDVI: NDVI plus terrain indicators and stratum; T: purely terrain indicators and stratum.

According to kappa statistic, a very good agreement (0.918, $p < 0.05$) was produced by the model with NDVI plus terrain parameters and stratum; substantial agreements (0.781 and 0.764, $p < 0.05$) were produced by the model with purely NDVI and the model with purely terrain indicators and stratum based on OAO scheme. Hence, the contribution of NDVI to explain soil texture class variability was explored by the relative improvement of classification accuracy of the model with NDVI plus terrain indicators and stratum over the model with purely terrain indicators and stratum. The relative improvements for clay, loam, and sand were 144%, 0%, and 14%, respectively. More samples of clay and sand were identified with the help of NDVI. This further confirmed the effects of soil texture on plant development. Soil texture directly determines the porosity of soil and hence affects its water-retention characteristics, nutrient-holding capacity, and soil fertility. Sandy soils tend to have relatively higher percentage of larger pores, whereas clayey soils tend to have relatively higher percentage of smaller pores. Therefore, clayey soils are often associated with poorly drained conditions with limited aeration for plant growth. It was found that crop yields reduced significantly when crops were grown in clayey soils [45]. Generally, loamy sand soils are suitable for root and tuber crop growth and development, because plants can get sufficient amounts of nutrients and consequently lead to higher yield [47].

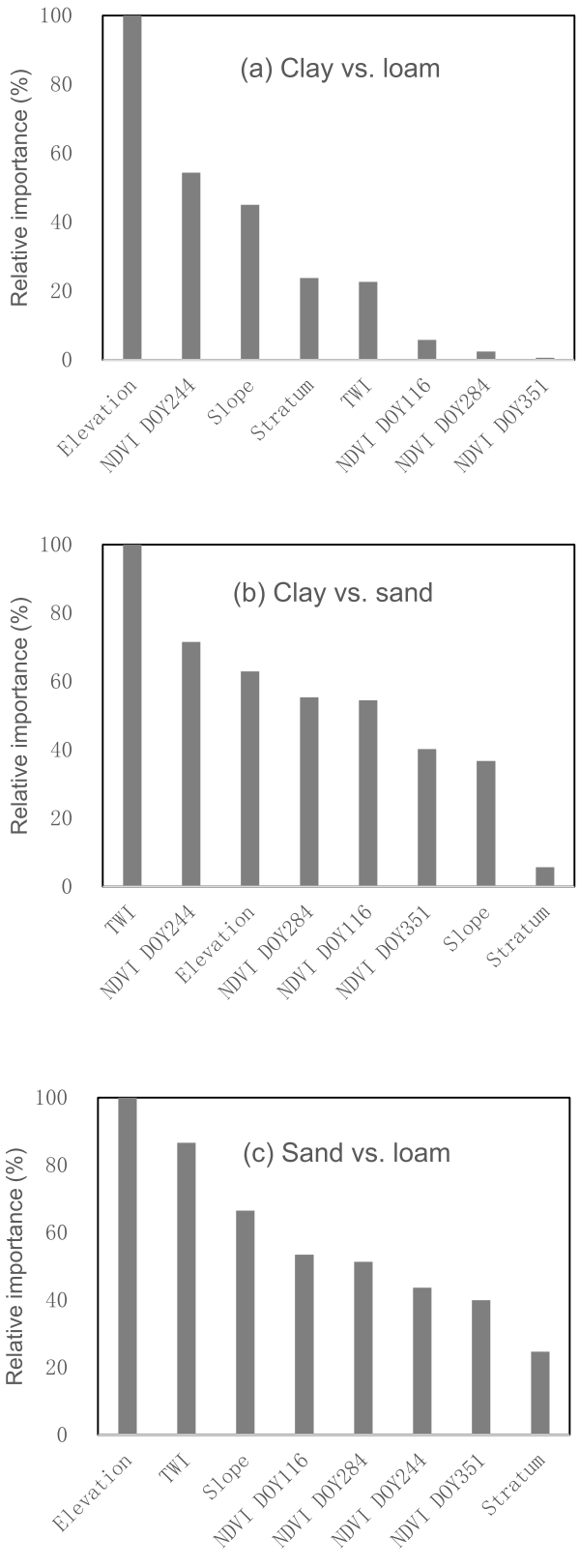

Fig. 5. Relative importance of factors to soil texture classes using CT model with OAO scheme. (a) Clay versus loam. (b) Clay versus sand. (c) Loam versus sand.

Furthermore, the accuracy indices produced by CT models using mixed pixels under the studied scenarios are also calculated and shown in Table VII. The models with pure pixels and with mixed pixels under each scheme gave similar overall accuracy values, but the models with pure pixels gave higher values of kappa index and AUC than the models with mixed pixels under each scheme. On average, the relative improvements in kappa index and AUC of the models with pure pixels over the models with mixed pixels were 38.5% and 5.8% under all-together scheme, 18.2% and 4.98% under OAA scheme, 8.6% and 5.03% under OAO scheme, respectively. In this case, the sample numbers of the three classes are unbalanced. About 81% of the samples were collected from loamy soils, 5.9% from clayey soils, and 13.1% from sandy soils. The overall accuracy index will be very high even most samples of clay and sand were misclassified into loam soil texture classes; for example, the models under all together and OAA schemes gave higher values of overall accuracy (Tables V and VI). Fortunately, kappa index and AUC are appropriate measures for handling imbalanced class problems [48]. The improvements of kappa and AUC of the models with pure pixels over the models with mixed pixels indicated that pixel purity was closely associated with model performance. This was in agreement with other studies [49], [50].

C. Relative Importance

The relative importance of NDVI, terrain indicators, and stratum was calculated using the CTs under OAO scheme (Fig. 5). The factors displayed varied relative weights for separating soil texture classes. The rank order was elevation > NDVI DOY 244 > slope > stratum > TWI > NDVI DOY116 > NDVI DOY 284 > NDVI DOY351 for clay versus loam strategy. The rank order was TWI > NDVI DOY 244 > elevation > NDVI DOY 284 > NDVI DOY 116 > NDVI DOY 351 > slope > stratum for clay versus sand strategy. The rank order was elevation > TWI > slope > NDVI DOY 116 > NDVI DOY 284 > NDVI DOY 244 > NDVI DOY 351 > stratum for loam versus sand strategy. Overall, terrain indicators had higher relative importance controlling the variability of soil texture classes. In lower areas, fields had higher water retaining capacity and thus gave rise to the occurrence of clayey soils [22], [25]. Besides, the lower relative importance of stratum to soil texture class variations could be attributed to the relationship between strata and topography (Table I). For the remote sensing imageries, NDVI measured at DOY 244 (September 1) in the stem and leaf growth period of sweet potatoes had higher relative importance for separating clayey soils from loamy and sandy soils [Fig. 5(a) and (b)]. This might be attributed to that root and tuber crops are more sensitive to soil texture [45]–[47].

V. Conclusion

Based on the common assumption that soil texture classes are closely related to environmental variables, such as topography, stratum, vegetation growth, and development. This paper investigated the usefulness of remote sensing imageries for identifying soil texture classes using classification methods. Classification strategy had great effects on the outputs. The models with OAO scheme obtained higher classification accuracy and kappa statistic than that with OAA and all-together schemes. For each classification scheme, the model with NDVI plus terrain indicators and stratum performed best with higher values of overall accuracy, kappa statistic, and AUC. Similar performance was produced by the model with purely NDVI parameters and the model with purely terrain indicators and stratum. More samples of clay and sand were identified with the help of NDVI. The contributions of NDVI to explain soil texture class variability were 144%, 0%, and 14% for clay, loam, and sand, respectively. The outcomes indicated that NDVI measured during the stem and leaf growth period of sweet potatoes was the most important period for identifying soil texture classes in the study area.

References

[1] B. G. Davey, "The chemical properties of soils," in *The Scientific Basis of Modern Agriculture*, K. O. Campbell and J. W. Bowyer, Eds. Sydney, NSW, Australia: Sydney Univ. Press, 1990, pp. 54–78.

[2] J. R. Irons, R. A. Weismiller, and G. W. Pterson, "Soil reflectance," in *Theory and Applications of Optical Remote Sensing*. New York, NY, USA: Wiley, 1989, pp. 66–106.

[3] F. A. Afshar, S. Ayoubi, A. A. Besalatpour, H. Khademi, and A. Castrignano, "Integrating auxiliary data and geophysical techniques for the estimation of soil clay content using CHAID algorithm," *J. Appl. Geophys.*, vol. 126, no. 3, pp. 87–97, Mar. 2016.

[4] T. J. Farrar, S. E. Nicholson, and A. R. Lare, "The influence of soil type on the relationships between NDVI, rainfall, and soil moisture in semiarid Botswana. II. NDVI response to soil oisture," *Remote Sens. Environ.*, vol. 50, no. 2, pp. 121–133, Nov. 1994.

[5] M. Stępień, S. Samborski, D. Gozdowski, E. S. Dobers, J. Chormański, and J. Szatyłowicz, "Assessment of soil texture class on agricultural fields using ECa, Amber NDVI, and topographic properties," *J. Plant Nutrition Soil Sci.*, vol. 178, no. 3, pp. 523–536, Jun. 2015.

[6] C. da Silva Chagas, W. de Carvalho, Jr., S. B. Bhering, and B. C. Filho, "Spatial prediction of soil surface texture in a semiarid region using random forest and multiple linear regressions," *Catena*, vol. 139, no. 4, pp. 232–240, Apr. 2016.

[7] H. Li *et al.*, "Multispectral reflectance of cotton related to plant growth, soil water and texture, and site elevation," *Agronomy J.*, vol. 93, no. 6, pp. 1327–1337, 2001.

[8] G. Ou and Y. L. Murphey, "Multi-class pattern classification using neural networks," *Pattern Recognit.*, vol. 40, no. 1, pp. 4–18, Jan. 2007.

[9] B. Ehret, "Pattern recognition of geophysical data," *Geoderma*, vol. 160, no. 1, pp. 111–125, Nov. 2010.

[10] C. W. Brungard, J. L. Boettinger, M. C. Duniway, S. A. Wills, and T. C. Edwards, Jr., "Machine learning for predicting soil classes in three semi-arid landscapes," *Geoderma*, vol. 239, no. 2, pp. 68–83, Feb. 2015.

[11] N. El-Bendary, E. El Hariri, A. E. Hassanien, and A. Badr, "Using machine learning techniques for evaluating tomato ripeness," *Expert Syst. Appl.*, vol. 42, no. 4, pp. 1892–1905, Mar. 2015.

[12] B. Heung, H. C. Ho, J. Zhang, A. Knudby, C. E. Bulmer, and M. G. Schmidt, "An overview and comparison of machine-learning techniques for classification purposes in digital soil mapping," *Geoderma*, vol. 265, no. 3, pp. 62–77, Mar. 2016.

[13] J. W. Rouse, Jr., R. H. Hass, J. A. Schell, and D. W. Deering, "Monitoring vegetation systems in the Great Plains with ERTS," in *Proc. 3rd Earth Resour. Technol. Satellite Symp. (ERTS)*, vol. 1, 1973, pp. 309–317. [Online]. Available: https://doi.org/citeulike-article-id:12009708

[14] A. Este, F. Gringoli, and L. Salgarelli, "Support vector machines for TCP traffic classification," *Comput. Netw.*, vol. 53, no. 14, pp. 2476–2490, Sep. 2009.

[15] D. Li, W. Yang, and S. Wang, "Classification of foreign fibers in cotton lint using machine vision and multi-class support vector machine," *Comput. Electron. Agricult.*, vol. 74, no. 2, pp. 274–279, Nov. 2010.

[16] A. Mathur and G. M. Foody, "Multiclass and binary SVM classification: Implications for training and classification users," *IEEE Geosci. Remote Sens. Lett.*, vol. 5, no. 2, pp. 241–245, Apr. 2008.

[17] R. Debnath, N. Takahide, and H. Takahashi, "A decision based one-against-one method for multi-class support vector machine," *Pattern Anal. Appl.*, vol. 7, no. 2, pp. 164–175, Jul. 2004.

[18] R. Taghizadeh-Mehrjardi, K. Nabiollahi, B. Minasny, and J. Triantafilis, "Comparing data mining classifiers to predict spatial distribution of USDA-family soil groups in Baneh region, Iran," *Geoderma*, vols. 253–254, no. 9, pp. 67–77, Sep. 2015.

[19] W. Wu, A.-D. Li, X.-H. He, R. Ma, H.-B. Liu, and J.-K. Lv, "A comparison of support vector machines, artificial neural network and classification tree for identifying soil texture classes in south-west China," *Comput. Electron. Agricult.*, vol. 144, no. 1, pp. 86–93, Jan. 2018.

[20] L. Breiman, J. H. Friedman, R. A. Olshen, and C. J. Stone, *Classification and Regression Trees*. Belmont, CA, USA: Wadsworth, 1984.

[21] D. E. Brown, V. Corruble, and C. L. Pittard, "A comparison of decision tree classifiers with backpropagation neural networks for multimodal classification problems," *Pattern Recognit.*, vol. 26, no. 6, pp. 953–961, Jun. 1993.

[22] A. Gobin, P. Campling, and J. Feyen, "Soil-landscape modelling to quantify spatial variability of soil texture," *Phys. Chem. Earth B, Hydrol., Oceans Atmos.*, vol. 26, no. 1, pp. 41–45, Jan. 2001.

[23] D. J. Brown, M. K. Clayton, and K. McSweeney, "Potential terrain controls on soil color, texture contrast and grain-size deposition for the original catena landscape in Uganda," *Geoderma*, vol. 122, no. 1, pp. 51–72, Sep. 2004.

[24] Z. Zhao, T. L. Chow, H. W. Rees, Q. Yang, Z. Xing, and F.-R. Meng, "Predict soil texture distributions using an artificial neural network model," *Comput. Electron. Agricult.*, vol. 65, no. 1, pp. 36–48, Jan. 2009.

[25] M. Ließ, B. Glaser, and B. Huwe, "Uncertainty in the spatial prediction of soil texture: Comparison of regression tree and Random Forest models," *Geoderma*, vol. 170, no. 1, pp. 70–79, Jan. 2012.

[26] Z. T. Gong, *Chinese Soil Taxonomy*, (in Chinese). Beijing, China: Science Press, 1999.

[27] J. G. Masek *et al.*, "A Landsat surface reflectance dataset for North America, 1990-2000," *IEEE Geosci. Remote Sens. Lett.*, vol. 3, no. 1, pp. 68–72, Jan. 2006.

[28] E. Vermote, C. Justice, M. Claverie, and B. Franch, "Preliminary analysis of the performance of the Landsat 8/OLI land surface reflectance product," *Remote Sens. Environ.*, vol. 185, no. 11, pp. 46–56, Nov. 2016.

[29] S. J. Thien, "A flow diagram for teaching texture-by-feel analysis," *J. Agronomic Educ.*, vol. 8, no. 2, pp. 54–55, Jan. 1979.

[30] *Guidelines for Soil Description*, FAO, Rome, Italy, 2006.

[31] H. Sponagel *et al.*, Eds., *Bodenkundliche Kartieranleitung* (German Manual of Soil Mapping, KA5), 5th ed. Hannover, Germany: Bundesanstalt für Geowissenschaften und Rohstoffe, 2005.

[32] J. E. Foss, W. R. Wright, and R. H. Coles, "Testing the accuracy of field textures," *Soil Sci. Sco. Amer. J.*, vol. 39, no. 4, pp. 800–802, 1975.

[33] D. F. Post, A. R. Huete, and D. S. Pease, "A comparison of soil scientist estimations and laboratory determinations of some Arizona soil properties," *J. Soil Water Conservation*, vol. 41, no. 6, pp. 421–424, Nov./Dec. 1986.

[34] Y. A. Pachepsky, W. J. Rawls, and H. S. Lin, "Hydropedology and pedotransfer functions," *Geoderma*, vol. 131, nos. 3–4, pp. 308–316, Apr. 2006.

[35] C. Vos, A. Don, R. Prietz, A. Heidkamp, and A. Freibauer, "Field-based soil-texture estimates could replace laboratory analysis," *Geoderma*, vol. 267, no. 4, pp. 215–219, Apr. 2016.

[36] O. Conrad *et al.*, "System for Automated Geoscientific Analyses (SAGA) v.2.1.4," *Geosci. Model Develop.*, vol. 8, no. 7, pp. 1991–2007, 2015.

[37] J. R. Quinlan, "Induction of decision trees," *Mach. Learn.*, vol. 1, no. 1, pp. 81–106, 1986.

[38] L. E. Raileanu and K. Stoffel, "Theoretical comparison between the gini index and information gain criteria," *Ann. Math. Artif. Intel.*, vol. 41, no. 1, pp. 77–93, May 2004.

[39] D. J. Brus, B. Kempen, and G. B. M. Heuvelink, "Sampling for validation of digital soil maps," *Eur. J. Soil Sci.*, vol. 62, no. 3, pp. 394–407, Jun. 2011.

[40] M. Sharma, P. Sharma, R. B. Pachori, and U. R. Acharya, "Dual-tree complex wavelet transform-based features for automated alcoholism identification," *Int. J. Fuzzy Syst.*, vol. 20, no. 4, pp. 1297–1308, Apr. 2018.

[41] I. Zlobec, R. Steele, N. Nigam, and C. C. Compton, "A predictive model of rectal tumor response to preoperative radiotherapy using classification and regression tree methods," *Clin. Cancer Res.*, vol. 11, no. 15, pp. 5440–5443, Aug. 2005.

[42] J. R. Landis and G. G. Koch, "The measurement of observer agreement for categorical data," *Biometrics*, vol. 33, no. 1, pp. 159–174, 1977.

[43] M. Kantardzic, *Data Mining: Concepts, Models, Methods, and Algorithms*. Hoboken, NJ, USA: Wiley, 2011.

[44] J. Nyiraneza, A. N. Cambouris, N. Ziadi, N. Tremblay, and M. C. Nolin, "Spring wheat yield and quality related to soil texture and nitrogen fertilization," *Agronomy J.*, vol. 104, no. 3, pp. 589–599, May/Jun. 2012.

[45] N. Katerji and M. Marcello, "The effect of soil texture on the water use efficiency of irrigated crops: Results of a multi-year experiment carried out in the Mediterranean region," *Eur. J. Agronomy*, vol. 30, no. 2, pp. 95–100, Feb. 2009.

[46] C. A. Redulla, J. R. Davenport, R. G. Evans, M. J. Hattendorf, A. K. Alva, and R. A. Boydston, "Relating potato yield and quality to field scale variability in soil characteristics," *Amer. J. Potato Res.*, vol. 79, no. 5, pp. 317–323, Sep.-Oct. 2002.

[47] S. H. Ahmadi *et al.*, "Interaction of different irrigation strategies and soil textures on the nitrogen uptake of field grown potatoes," *Int. J. Plant Prod.*, vol. 5, no. 3, pp. 263–274, Jul. 2011.

[48] J. Huang and C. X. Ling, "Using AUC and accuracy in evaluating learning algorithms," *IEEE Trans. Knowl. Data Eng.*, vol. 17, no. 3, pp. 299–310, Mar. 2005.

[49] C. E. Woodcock and A. H. Strahler, "The factor of scale in remote sensing," *Remote Sens. Environ.*, vol. 21, no. 3, pp. 311–332, Apr. 1987.

[50] Y. Chen, Y. Ge, G. B. M. Heuvelink, J. Hu, and Y. Jiang, "Hybrid constraints of pure and mixed pixels for soft-then-hard super-resolution mapping with multiple shifted images," *IEEE J. Sel. Topics Appl. Earth Observ. Remote Sens.*, vol. 8, no. 5, pp. 2040–2052, May 2015.

Wei Wu received the Ph.D. degree in agriculture from Southwest University, Chongqing, China, in 2007.

She is currently a Professor with the College of Computer and Information Science, Southwest University. Her research interests include computational intelligence with applications to decision support, data mining, and image understanding.

Qipo Yang received the bachelor's degree in agricultural resources and environment from Henan Agricultural University, Zhengzhou, China, in 2016. He is currently pursuing the master's degree with the Chongqing Key Laboratory of Digital Agriculture, Chongqing, China.

His research interests include remote sensing application in agriculture and precision agriculture in hilly areas.

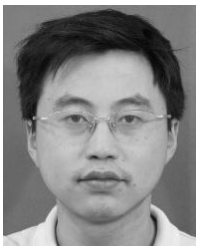

Jiake Lv received the Ph.D. degree in utilization science of agricultural resources from Southwest University, Chongqing, China, in 2010.

He is currently an Associate Professor with the College of Computer and Information Science, Southwest University. His research interests include computer education, intelligent data modeling, and environment geographic information system.

Aidi Li, photograph and biography not available at the time of publication.

Hongbin Liu received the Ph.D. degree in utilization science of agricultural resources from Southwest University, Chongqing, China, in 2002.

He is currently a Professor with the College of Resources and Environment, Southwest University. His research interests include the impacts of environmental factors, such as topography, soil, and climate, on crop growth and development, and the development of predictive models for improving the understanding of the relationships between topography and soil properties based on the technologies of geographical information system and remote sensing.